agriculture

MDPI

Article

Konjac Glucomannan Oligosaccharides (KGMOS) Confers Innate Immunity against *Phytophthora nicotianae* in Tobacco

Md Mijanur Rahman Rajib [1,2,3], Kuikui Li [1], Md Saikat Hossain Bhuiyan [1,2,4], Wenxia Wang [1], Jin Gao [1] and Heng Yin [1,2,*]

[1] Dalian Engineering Research Center for Carbohydrate Agricultural Preparations, Dalian Technology Innovation Center for Green Agriculture, Liaoning Provincial Key Laboratory of Carbohydrates, Dalian Institute of Chemical Physics, Chinese Academy of Sciences, Dalian 116023, China; mmrrajib@bsmrau.edu.bd (M.M.R.R.); lkk@dicp.ac.cn (K.L.); saikat@dicp.ac.cn (M.S.H.B.); wangwx@dicp.ac.cn (W.W.); gaojin0903@dicp.ac.cn (J.G.)
[2] University of Chinese Academy of Sciences, Beijing 100190, China
[3] Department of Horticulture, Bangabandhu Sheikh Mujibur Rahman Agricultural University, Gazipur 1706, Bangladesh
[4] Bangladesh Institute of Nuclear Agriculture, Mymensingh 2202, Bangladesh
* Correspondence: yinheng@dicp.ac.cn; Tel.: +86-(0411)-84379061; Fax: +86-(0411)-8437906

Abstract: In this study, KGMOS (DP, 2-13), derived from KGM (Konjac glucomannan), was applied to elucidate plant immunity in a *Nicotiana benthamiana Phytophthora nicotianae* model. Application of KGMOS (25–100 mg/L) notably inhibited *P. nicotianae*, resulting in reduced disease indices and a significant accumulation of defense molecules such as H_2O_2 and callose. Transcriptomic analysis revealed that genes shared between KGMOS-treated and control plants are involved in signaling pathways, transcription regulation, hydrogen peroxide catabolism, and oxidative stress response. This suggests that KGMOS triggers H_2O_2 accumulation, callose deposition, and activation of the salicylic acid (SA) and jasmonic acid/ethylene (JA/ET) pathways after pathogen inoculation. Upregulated defense-response genes in the KGMOS group included SA-related late blight-resistant, pathogenesis-related (*PR*), and JA/ET-related ethylene response factor (*ERF*) genes. Heatmap analysis showed more upregulated defense genes (*PR* and *NPR*) related to SA in the KGMOS-treated group than in controls. RT-qPCR validation revealed significant upregulation of SA and JA/ET pathway genes in KGMOS-treated plants. Higher SA content in these plants suggests enhanced disease resistance. This study concludes that KGMOS pre-treatment induced resistance against *P. nicotianae*, especially at a lower concentration (25 mg/L). These findings could offer valuable insights for the future application of KGMOS in controlling plant diseases for sustainable agriculture and postharvest management.

Keywords: KGMOS; transcriptome; phytophthora nicotianae; nicotiana benthamiana

check for updates

Citation: Rajib, M.M.R.; Li, K.; Bhuiyan, M.S.H.; Wang, W.; Gao, J.; Yin, H. Konjac Glucomannan Oligosaccharides (KGMOS) Confers Innate Immunity against *Phytophthora nicotianae* in Tobacco. *Agriculture* **2024**, *14*, 1289. https://doi.org/10.3390/agriculture14081289

Academic Editor: Filippo De Curtis

Received: 27 June 2024
Revised: 30 July 2024
Accepted: 2 August 2024
Published: 5 August 2024

Copyright: © 2024 by the authors. Licensee MDPI, Basel, Switzerland. This article is an open access article distributed under the terms and conditions of the Creative Commons Attribution (CC BY) license (https://creativecommons.org/licenses/by/4.0/).

1. Introduction

Sustainable crop management necessitates a comprehensive understanding of plant defense mechanisms, as biotic diseases cause a significant loss in both crop fields and natural ecosystems. Through interaction with pathogens, plants have evolved immunomodulatory strategies against diverse pathogens over evolutionary time [1]. Plant immunity is activated by interacting with receptors on the cell surface and inside the cells to cope with pathogen invasion [2]. These receptors recognize pathogen molecules and initiate a defense response, such as the production of antimicrobial compounds or the activation of immune cells. Pattern-triggered immunity (PTI) is initiated when the pattern recognition receptor (PRR) recognizes conserved microbial patterns, triggering low-level immunity cascades to limit nonadaptive pathogen growth. The pathogen secretes effectors into host cells to suppress first-line immunity and boost virulence by targeting organelles and signaling nodes. Effector-triggered immunity (ETI) is triggered by nucleotide-binding leucine-rich

repeat (NLR) proteins that recognize pathogen effectors [3]. ETI alters intracellular traffic, increases signaling cascades, and causes localized cell death, finally enhancing basal immunity [4].

The two-tiered plant immune system initiates PTI and ETI through intellectually different frameworks and reveals mutual interaction between them in a zig-zag–zig model [5]. In recent years, some researchers have investigated whether ETI enhances PTI by interacting with its components [6]. In parallel with the early signaling molecules, PTI and ETI ultimately converge into a number of similar downstream responses, although they differ in terms of amplitudes and dynamics [7]. Even though PTI and ETI are different, these two immune systems also partially overlap in downstream responses, including MAPK cascades, calcium signal inflow (Ca^{2+}), reactive oxygen species (ROS) bursts, transcriptional reprogramming, callose deposition, accumulation of phytohormone signaling, and PR proteins [8–10]. The accumulation of SA, activation of *PR*, and *non-expressor of PR1* (*NPRI*) genes play a crucial role in establishing systemic acquired resistance (SAR) [11,12]. In contrast, induced systemic resistance (ISR) is closely related to the JA/ET pathway and is triggered in the presence of necrotrophic pathogens [13]. The intricate interplay of these diverse pathways, genes, and PR protein families exemplifies the sophisticated defense strategies employed by plants in response to pathogenic challenges [14,15].

P. nicotianae, the causative agent of tobacco black shank, poses more than 100 species that significantly threaten 255 genera of 90 families (predominately solanaceous) [16], resulting in devastating diseases affecting various plants [17]. The disease manifests as root rot, stem necrosis, wilting, and chlorosis, leading to considerable yield loss, quality reduction, and even death [18–20]. The high adaptability and diversity of *P. nicotianae* make it difficult to control in nature. Additionally, the secreted effectors from pathogens also pose challenges to host resistance [21,22]. Hence, it is imperative to establish a sustainable plant protection system that is safe, efficient, and environmentally friendly to combat these crises.

Natural elicitors of plant immunity reduce the detrimental moieties of hazardous chemicals by activating and priming immunity [23]. These biological elicitors are classified into proteins, oligosaccharides, glycopeptides, lipids, lipopeptides, small molecule metabolites, and chemical compounds [24]. A diverse range of biocontrol strains and natural agents (secondary metabolites) are also effective in combating *P. nicotianae* by activating PTI and ETI [25–27]. Moreover, the degradation products of some plant storage polysaccharides have been found to elicit plant immunity and function as functional carbohydrates. The elicitor activities of these oligosaccharides have recently attracted considerable attention in the field of immunity. Fructo-oligosaccharides (FOS) extracted from burdock root (*Arctium lappa*) induced resistance in cucumber against a number of fungal diseases, such as *Colletotrichum lagenarium* [28], *Sphaerotheca fuliginea* [29], and *Botrytis cinerea* [30]. Meanwhile, FOS not only induced resistance against the tobacco mosaic virus in tobacco [31] but also reduced *Botrytis cinerea* infection in grapes, kiwifruit, and tomatoes; *Penicillium expansum* in apples; *P. italicum* in citrus; *C. musae* in bananas [32]; and *Rhizopus* and *P. expansum* (blue mold) in peaches [33]. FOS activated and accumulated downstream signaling molecules, secondary metabolites, SA content, and *PR* genes to enhance disease resistance to these pathogens [34]. On the other hand, mannan oligosaccharides (MOS) are hydrolyzed upon locust bean gum, significantly enhancing intracellular Ca^{2+} and ROS generation [35]. In rice and tobacco, MOS was found to exhibit antimicrobial activity against *Xanthomonas oryzae* and *P. nicotianae* via SA and JA-related pathways, respectively [35]. These reports highlighted the capacity of storage polysaccharide-derived oligosaccharides to induce immunity by activating signaling molecules associated with PTI such as ROS, NO, and Ca^{2+} at an early stage. This is followed by the induction of secondary signaling metabolites related to ETI and SAR, including SA, the activation of defense-related genes, and the accumulation of PR proteins, along with JA and ET related to ISR.

These kinds of literature achievements focus our present study on another storage polysaccharide-derived oligosaccharide, konjac glucomannan oligosaccharides (KGMOS).

So far, KGMOS has been reported to inhibit the proliferation of pathogenic fungi (*Candida albicans*) and bacteria (*Propionibacterium acnes*) as well as spore-forming bacteria (*Bacillus*, *Clostridium*) [36]. Simultaneously, KGMOS exhibited intestinal immunity by inhibiting populations and hazardous activities of pathogenic bacteria like *Escherichia coli*, *Salmonella enteritidis*, *Vibrio parahemolyticus*, *Staphylococcus aureus*, and *Aeromonas hydrophila* in humans [37,38], fish [39], and animals [40,41]. These researchers revealed that KGMOS inhibited harmful microbial cells, scavenged free radicals (ROS) and Ca^{2+}, activated anti-inflammatory activity, and modulated the systemic immune system. This suggests that KGMOS might have the ability to induce plant immunity through PTI, ETI, SAR, or ISR pathways. However, it is still not clear whether KGMOS functions as an elicitor of plant immunity, indicating the necessity for further research. Additionally, KGMOS is gaining interest due to its cost-effectiveness, higher water solubility and absorption capacity, biodegradability, and eco-friendly biostimulant capacity for enhancing plant and soil health. Hence, our laboratory developed a counterpart, KGMOS, to discover more effective alternatives for enhancing plant immunity.

In this study, we pre-treated tobacco plants with diverse concentrations of KGMOS to assess their disease resistance to *P. nicotianae*, simultaneously measuring defense-related signaling molecules and hormones and detecting the expression of relevant genes within the *N. benthamiana-P. nicotianae* system. Meanwhile, a comparative transcriptomic analysis was also conducted to explore how tobacco responded to *P. nicotianae* infection after being pre-treated with KGMOS. Our investigation aspired to gain a deeper understanding of the intricate mechanisms by which KGMOS contributes to plant disease resistance.

2. Materials and Methods

2.1. Preparation of KGMOS

In our laboratory, KGMOS were synthesized through the enzymatic hydrolysis of konjac glucomannan (KGM) storage polysaccharide. The enzyme β-1,4-mannanase (*Pp*ManA) from *Paenibacillus polymyxa* rhizobacterium was employed to liberate a range of KGMOS (DP, 2-13). All materials and chemicals, except the RNA extraction kit and qPCR mix, were of analytically pure grade and obtained from Sinopharm Chemical Reagent Co., Ltd. (Shanghai, China). The extraction kit and qPCR mix were steady pure grade and were, respectively, from Accurate Biotechnology (Hunan) Co., Ltd., Hunan, China and Mona Biotechnology Co., Ltd., Suzhou, China.

2.2. Plant Materials and Treatments

N. benthamiana seeds were surface sterilized with 5% (*w*/*v*) sodium hypochlorite for 5 min, followed by three washes with sterilized water. Subsequently, the seeds were spread out on a plastic pot containing autoclaved media and incubated in a growth chamber with a 16/8 h light/dark cycle at 25 °C. After 10 days, the *N. benthamiana* seedlings were transferred into plastic pots filled with a mixture of sterilized loamy soil and vermiculite (1:1) and kept in the greenhouse, maintaining the same conditions as the growth chamber. Once the seedlings reached 4 weeks old, uniform and robustly grown plants were selected for pre-treatment. Building on previous research from our laboratory, this pre-treatment involved spraying water (control) and various concentrations of KGMOS (25, 50, and 100 mg/L) on the seedlings. Following the pre-treatment, *P. nicotiana* was inoculated within 24 h to assess plant resistance. The adaxial center of the second leaf from the bottom was lightly scraped to create a 2 mm diameter area. A drop of water was added to the scraped spot, followed by the placement of a fungal disk. The inoculated leaf was then completely wrapped with a transparent polyethylene sheet. Finally, the entire tray of inoculated plants was placed under a plastic cover and grouped to maintain a homogeneous, hot, and humid environment. The experimental groups were categorized as follows: the mock group comprised plants sprayed solely with water, followed by the control group (CK) subjected to fungal inoculation. Meanwhile, plants treated with KGMOS were allocated to

the KGMOS group. Each treatment in each group consisted of a minimum of 10 plants and was repeated three times.

2.3. Culture and Inoculation of Pathogen

P. nicotiana was cultured on Petri dishes, each filled with 10 mL of potato dextrose agar (PDA comprising potato infusion powder 4 g, sucrose 20 g, and agar 15 g, pH 5.6, in 1 L), and maintained at 28 °C for 10 days. Once the mycelia of *P. nicotianae* completely covered the PDA plate, a sterile puncher with a 5 mm diameter was employed to collect fungal samples. Subsequently, the obtained fungus disk was positioned at the center of a Petri dish containing 10 mL PDA, containing different concentrations of KGMOS in accordance with the treatments, with four replications for the antifungal test. KGMOS was dissolved in sterile water and incorporated into an autoclaved PDA medium just before pouring into Petri dishes under a laminar airflow chamber. The chemical fungicide carbendazim 50% @ 1 g/L (Sichuan Runner Technology Co., Ltd., Chengdu, China) was used as a positive control (PC). All inoculated plates were then incubated in a chamber at 28 °C for 7 days, and the fungal diameter was monitored daily. Likewise, the fungus disk was applied at the center of a selected leaf from each plant through scraping. The inoculated leaves of plants were subsequently positioned on moist paper, and all plants were enclosed in a humid chamber for 72 h. After this period, the plants were transferred to the greenhouse condition again, photographed for disease area, and measured using ImageJ software 1.52a by National Institure of Health, USA.

2.4. Detection of H_2O_2 and Callose Molecules

Hydrogen peroxide (H_2O_2) was assayed 24 h after *P. nictotianae* inoculation in the *N. benthamiana* plant cultivated under the previously mentioned in situ conditions. In situ detection of ROS (H_2O_2) burst was performed following an earlier reference with modifications [42]. Briefly, for each treatment, six 4-week-old plants were treated with sterile water and the indicated compounds, KGMOS (25, 50, and 100 mg/L). At 24 h after treatment, six leaves from six plants in each treatment group were inoculated with the fungus and kept in a high-humidity chamber for another 24 h, as mentioned earlier. Two disks near the adaxially infected area were then punched from each infected leaf. The collected disks were transferred into separate flasks, each covered with aluminum foil and containing 25 mL of staining solution. Then, leaf disks were gently vacuum-infiltrated (15 min) with 1 mg/mL 3,3′-diaminobenzidine (DAB) dissolved in 200 mM sodium phosphate buffer (pH 3.0) and 0.05% (*v*/*v*) Tween 20. The staining reaction was terminated 5 h after DAB infiltration in a shaker (dark), and leaf disks were boiled to remove chlorophyll and fixed in 25 mL of a preservative solution composed of ethanol–glycerol–acetic acid (3:1:1). Pictures were taken with a camera, and the intensity was analyzed by ImageJ software. The 8-bit images were calibrated to uncalibrated optical density (OD) to measure the intensity.

After 72 h of fungal inoculation, leaf disks near the adaxial infected area were delicately collected for callose determination following the previously described protocol with modifications [43]. To eliminate chlorophyll from these disks, they were emersed in 30 mL of 95% ethanol in separate flasks and agitated for 24 h at room temperature. Subsequently, leaf disks were rinsed in 150 mM K_2HPO_4 for 30 min. The disks were then incubated in a 25 mL solution consisting of 150 mM K_2HPO_4 and 0.01% aniline blue (diphenylamine blue) for a minimum of 2 h within a 50 mL conical flask shielded with aluminum foil for light protection. To enhance the observation time and minimize the interference of air bubbles, the disks were embedded in 150 mM K_2HPO_4 again with 50% glycerol before further analysis. Callose depositions were measured by using fluorescence microscopy at a wavelength of 370 nm, with a maximum emission wavelength of 509 nm. Photographs were captured, and the intensity was analyzed using ImageJ software. The 8-bit images were calibrated with step-tablet OD calibration to measure the intensity.

2.5. RNA Extraction, cDNA Library, RT-qPCR, and Transcriptomic Analysis

RNA extraction from frozen leaves was performed using Trizol (Beijing Lablead Biotech Co., Ltd.) in adherence to the guidelines provided by the manufacturer (Accurate Biotechnology Co., Ltd., Hunan). The quantification of RNA was conducted through Scandrop 100 (Analytik Jena AG, Germany). The GoScriptTM Reverse Transcription Mix (Promega, USA) was utilized for the conversion of an equivalent RNA amount into cDNA. Following transcription, the cDNA underwent dilution and was subsequently employed for q-PCR analysis, conducted on the qTOWER 2.2 instrument (Analytik Jena AG, Germany). The reaction volume, set at 20 µL, included cDNA dilutions, qPCR mix (MonAmpTM ChemoHS qPCR Mix, Monad), and gene-specific primers. The assessment of gene expression levels relative to *actin2* was performed with the $2^{-\Delta\Delta Ct}$ method [44]. The primer sequences are provided in Supplementary Table S1.

Differentially expressed genes (DEGs) were identified based on the criteria of $\log_2$ (fold change) > 1 and Q value $\leq$ 0.05. The Q value, which represents the False Discovery Rate (FDR) adjusted *p*-value, is used to determine significance. A Q value $\leq$ 0.05 is generally considered indicative of significant enrichment. The clean data (removing connectors and unknown and low-quality bases) were then analyzed to perform functional annotation of DEGs in BGI Dr. Tom's software's DNBSEQ platform (https://biosys.bgi.com (accessed on 10 June 2024)). The analysis of DEGs was performed through the Kyoto Encyclopaedia of Genes and Genomes (KEGG) pathway, Gene Ontology (GO) functional enrichment analysis, and reference genome sequence (https://www.ncbi.nlm.nih.gov (accessed on 10 June 2024)). Different enriched pathways and biological and molecular processes related to plant immunity were identified as key parameters. These include MAPK signaling, phenylpropanoid biosynthesis, phenylalanine metabolism, plant–pathogen interactions, plant hormone signal transduction, response to hydrogen peroxide, and defense response genes associated with the SA, JA, and ET pathways.

2.6. Quantification of SA by LC–MS

LC–MS was used to quantify SA in frozen infected leaves (72 h) of *N. benthamiana* that were extracted using isopropanol, water, and hydrochloric acid (HCl) in 2:1:0.002 buffer [45]. The chromatographic conditions were adjusted by employing a Hypercarb column (Thermo Fisher, 150 mm × 2.1 mm, 5 µm) at 35 °C and 0.1% formic acid (A) adjusted to pH 9 with ammonium hydroxide and acetonitrile (B) eluted at 0.2 mL per minute. The gradient conditions were 0 min, 90% A + 10% B, 10 min, 40% A + 60% B, 14 min, 40% A + 60% B, 14.1 min, 90% A + 10% B, and 20 min, 90% A + 10% B. A Q-trap 5500 (AB SCIEX, USA) was used for SA detection.

3. Results

3.1. KGMOS Inhibited the Growth of P. nicotianae

To investigate the function of KGMOS on *P. nicotianae*, the tobacco leaves were pre-treated with different concentrations of KGMOS (ranging from 25, 50, and 100 mg/L) and then inoculated by *P. nicotianae*. Plants pre-treated with KGMOS exhibited a significant reduction in necrosis symptoms compared to control (Figure 1A), accompanied by a corresponding decrease of 16.5% to 30% in the final disease index (Figure 1B and Supplementary Table S2). The optimal concentration, identified as 25 mg/L, demonstrated a notable reduction in the spread of necrotic symptoms. At this concentration, the disease index for KGMOS was significantly lower than the control and the other two KGMOS (50 and 100 mg/L) pre-treatments (Figure 1B and Supplementary Table S2).

To verify whether KGMOS directly inhibited fungal growth, a pathogen inhibition experiment was conducted. A decline in fungal growth was observed in PDA plates treated with KGMOS for up to 7 days after inoculation (DAI) (Figure 1C). Initially, there were no notable differences within the first two days post-inoculation. However, in the subsequent three days following exposure, a significant increase in antifungal activity emerged. This trend continued up to 4 to 5 DAI, followed by a decline. Notably, when

KGMOS was applied at 25 mg/L, a higher inhibition rate and antifungal consistency were noted (Figure 1D). Our data demonstrated that KGMOS exhibited direct antifungal resistance ranging from 9.4% to 14.4% (Supplementary Table S2).

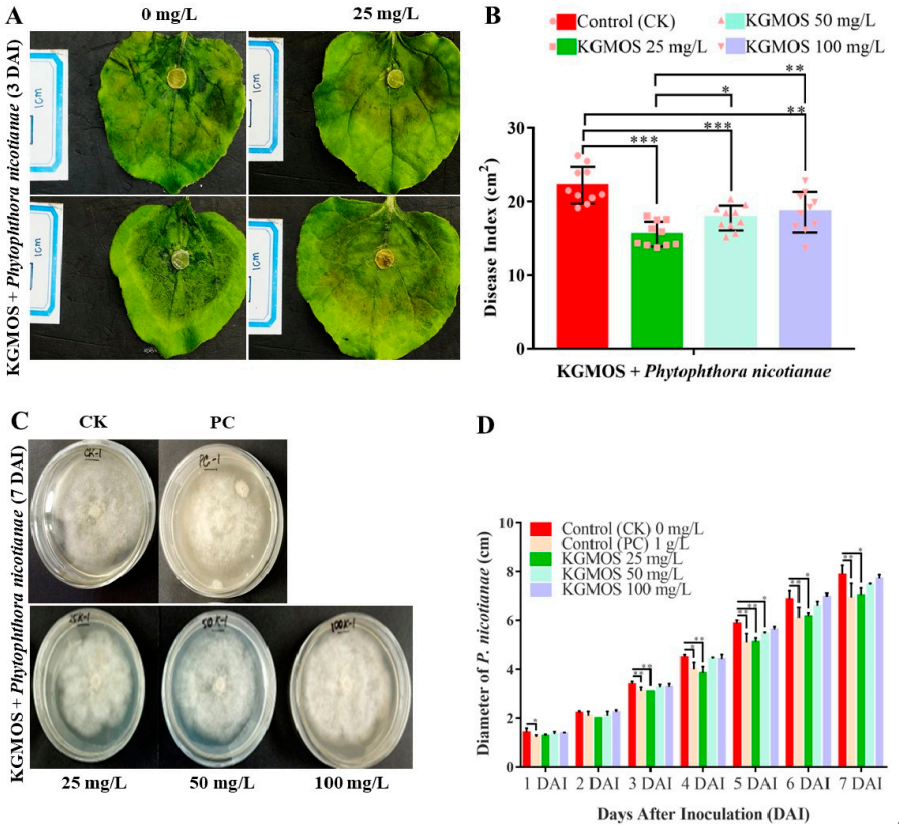

Figure 1. KGMOS-mediated disease resistance and fungal inhibition in *N. benthamiana*. (**A**) Disease symptoms in tobacco leaves under control and KGMOS treatments. (**B**) Disease index of KGMOS pre-treated and non-treated infected leaves. (**C**) Mycelial growth of *P. nicotianae* under control and KGMOS treatments. (**D**) Antifungal activity by KGMOS and control treatments. CK = control (sterilized water), PC = positive control (carbendazim 50% @ 1 g/L). Values are presented as the means ± SD of three independent measurements. IBM software SPSS (version 22) was used to analyze data, and means were compared with LSD at 0.05. Asterisks indicate significant differences (* $p < 0.05$, ** $p < 0.01$, *** $p < 0.001$).

3.2. KGMOS Elicited Accumulation of H_2O_2 and Callose Molecules

After 24 h of inoculation with *P. nicotianae* on pre-treated plants, the DAB staining assay was performed to evaluate the long-term generation of H_2O_2. The detection levels were notably elevated in the infected leaf disks treated with KGMOS compared to the mock group (Figures 2A and S1A). This finding indicates that the defense responses mediated by KGMOS might be regulated in an H_2O_2-dependent manner. Higher intensities were observed at a lower concentration (25 mg/L) of KGMOS pre-treatment, while intensities decreased with increasing concentrations up to 100 mg/L yet remained higher than the control (Figure 2B). The average optical density at 25 mg/L was 1.43 and 2.73-fold higher than control and mock, respectively.

Callose deposition was examined under a fluorescence microscope 72 h post-inoculation. All plants pre-treated with KGMOS (at concentrations of 25, 50, and 100 mg/L) exhibited higher callose deposition compared to the control plants (CK). Callose deposition demonstrated a negative correlation with the concentration of KGMOS, with lower concentrations displaying a higher number of callose depositions. Notably, 25 mg/L exhibited the highest

number of callose accumulations compared to other treatments (Figures 2C and S1B). The average at 25 mg/L for KGMOS was 1.86-fold higher (Figure 2D) than the control.

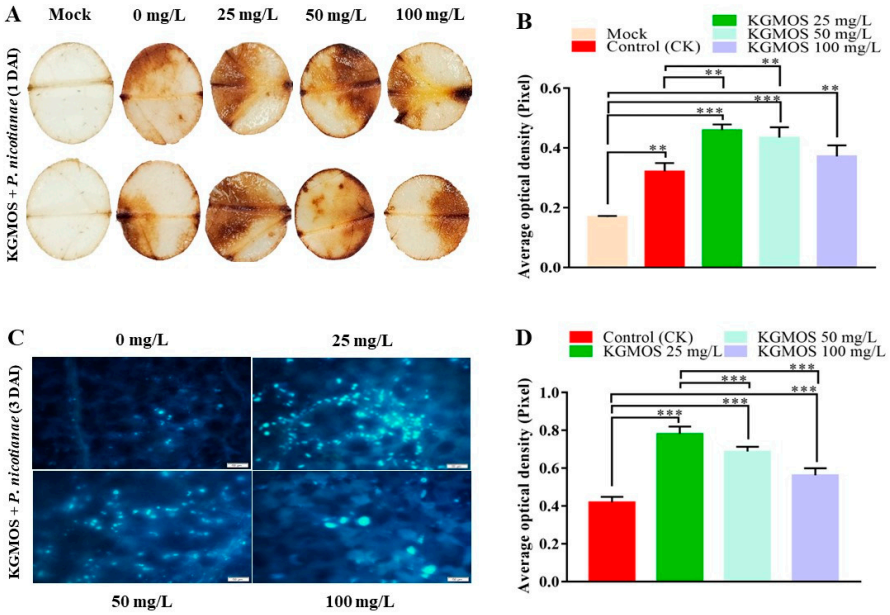

Figure 2. KGMOS induced H_2O_2 and callose deposition in *N. benthamiana*. (**A**) The ROS in leaves through DAB staining. (**B**) Average optical density of H_2O_2 accumulation. (**C**) Callose deposition in leaves through aniline blue staining. Scale bar—50 µm. (**D**) Average optical density of callose molecules. Values are presented as the means ± SD from three technical replicates. IBM software SPSS (version 22) was used to analyze data, and means were compared with LSD at 0.05. Asterisks indicate significant differences (** $p < 0.01$; *** $p < 0.001$).

3.3. Transcriptomic Analysis Triggered by KGMOS after P. nicotianae Infection

To obtain a comprehensive understanding of the mechanism underlying KGMOS-mediated *P. nicotianae* disease resistance, leaves pre-treated with 25 mg/L KGMOS and infected with *P. nicotianae* were selected for comparative transcriptome analysis at 3 DAI. Transcriptomic differences between the mock vs. KGMOS (PK) and mock vs. control groups (PC) were compared. Differentially expressed genes (DEGs) were identified using criteria of [log2(fold change) > 1] and *p*-value < 0.05. Among these DEGs, the volcano plot indicated 6673 genes were upregulated and 5111 genes were downregulated in KGMOS-treated leaves compared to the mock, while 6253 genes were upregulated and 4926 genes were downregulated in pathogen infection without KGMOS pre-treatment compared to the mock (Figure 3A,B). It appeared that a greater number of DEGs were upregulated and downregulated in the KGMOS group than in the control group after infection. This suggests that tobacco plants underwent a series of alterations in gene expression following *P. nicotianae* infection, with a higher degree of alternation in KGMOS-treated plants.

KEGG pathway enrichment analysis of the upregulated DEGs revealed their significant involvement in key resistance pathways, including "oxidative phosphorylation, plant–pathogen interaction, phenylpropanoid biosynthesis, MAPK signaling pathway, biosynthesis of amino acids, and carbon metabolism" (Figure 3C,D). This indicates that plant resistance against pathogens is activated through similar pathways in both KGMOS-treated and control groups. Consequently, 8876 DEGs were overlapped between KGMOS and control (Figure 3E). GO annotation of these overlapping DEGs highlighted a predominance of protein phosphorylation (513) and phosphorylation (644), along with other defense-related pathways (Figure 3F). These phosphorylation processes further validated the activation of the "MAPK signaling, plant–pathogen interaction, and plant hormone signal transduction" pathways (Figure S2A,B). Notably, a considerable number of DEGs were involved in these pathways in the KGMOS-treated group compared to the control

(Supplementary Table S3). The higher involvement of genes related to peroxidase enzymes suggests increased H_2O_2 production, callose deposition, and lignification. Conversely, downregulated DEGs were associated with pathways related to plant hormone signal transduction, photosynthesis, photosynthesis-antenna proteins, carotenoid biosynthesis, and various metabolic processes, particularly starch and sugar metabolism (Figure S2C,D). These findings suggest that the plants mediate the defense response by regulating defense-related pathways such as MAPK, plant hormone signaling, and certain biological and metabolic activities when tobacco was infected by *P. nicotianae*.

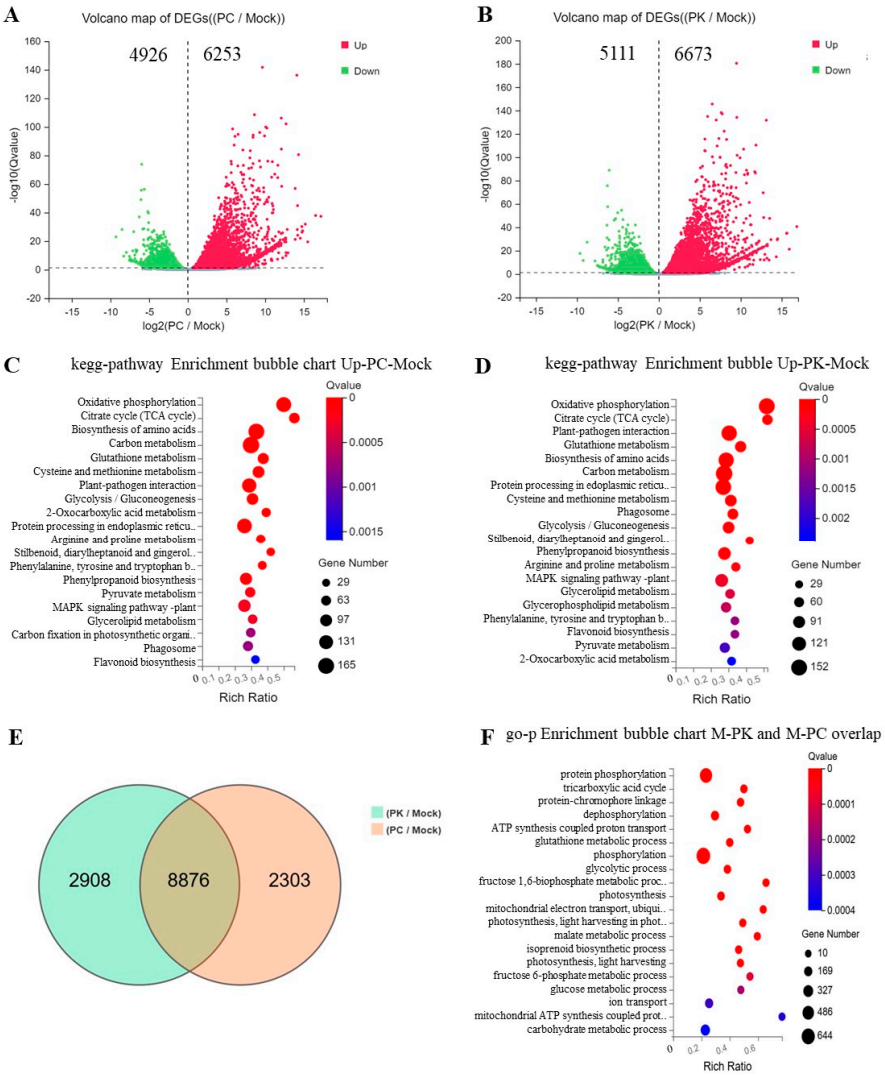

Figure 3. DEGs from *N. benthamiana* at 3 days after *P. nicotianae* infection. (**A**) Volcano plot displaying DEGs of the control group (PC) compared to the mock group. (**B**) Volcano plot displaying DEGs of the KGMOS group (PK) compared to the mock group, identified with [log2(fold change) > 1] and p-value < 0.05. (**C**) KEGG enrichment analysis of upregulated DEGs between the control and mock groups. (**D**) KEGG enrichment analysis of upregulated DEGs between the KGMOS and mock groups. (**E**) Distinct and overlapped DEGs in between the PK/mock and PC/mock groups. (**F**) GO annotation of overlapped DEGs between PK/mock and PC/mock. The horizontal axis represents the rich ratio, while the vertical axis represents the pathway names. Gene number: DEGs number; Q value: False discovery rate (FDR) adjusted p-value. Generally, a Q value ≤ 0.05 is regarded as a significant enrichment.

To determine the individual involvement of distinct and shared genes in each group, a Venn diagram was created comparing the mock, control, and KGMOS-treated groups.

This showed the density distribution of unique and shared genes among the three groups after pathogen infection. Following pathogen infection, gene expression profiling revealed that 710 genes in the KGMOS group and 978 genes in the control group were distinct, whereas 1504 genes were shared between the treated and non-treated control groups (Figure S3A). KEGG pathway enrichment showed that the distinct genes of both KGMOS and control groups were correlated with pathways such as "pentose and glucuronate interconversions and phenylpropanoid biosynthesis", which is involved in the synthesis of SA, with almost the same number of genes (12) in each pathway (Figure 4A,B). These data indicate that plants promote disease resistance to *P. nicotianae*, which might be dependent on the SA pathway. The KEGG pathway of the majority of the shared genes between KGMOS and the control group was composed of resistance pathways such as "phenylpropanoid biosynthesis (31 genes), the MAPK signaling pathway (20 genes), plant hormone signal transduction (22 genes), flavonoid biosynthesis (10 genes), and nitrogen metabolism" (9 genes) (Figure 4C). Moreover, GO enrichment analysis indicated that "defense response, ethylene-activated signaling pathway, regulation of transcription, DNA-templating, hydrogen peroxide catabolic process, and response to oxidative stress were associated with these shared genes of KGMOS and control after post-inoculation (Figure 4D). These results indicate that pathogen inoculation leads to H_2O_2 accumulation, callose deposition, and activation of the SA and JA/ET pathways.

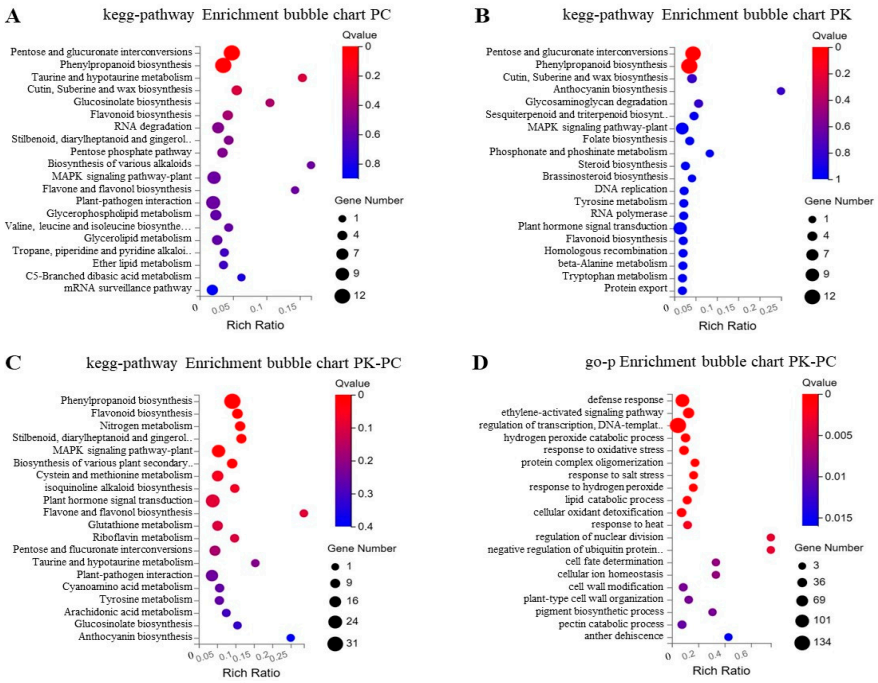

Figure 4. Transcriptomic analysis of distinct and overlapped genes in mock, control, and KGMOS groups. (**A**) KEGG pathway of unique genes in the control group (PC). (**B**) KEGG pathway of unique genes in the KGMOS group (PK). (**C**) KEGG pathway analysis of overlapped genes between control and KGMOS. (**D**) GO enrichment analysis of overlapped genes between control and KGMOS. The horizontal axis represents the rich ratio, while the vertical axis represents the pathway names. Gene number: DEGs number; Q value: FDR adjusted *p*-value.

To further investigate the expression differences in defense-response genes (94 genes) among mock (M), control (PC), and KGMOS pre-treatment (PK), an analysis was performed. The $\log_2$ (PK/PC) value demonstrated that 25 defense genes were upregulated after pathogen infection in the KGMOS group (Supplementary Table S4). The upregulation-dominated genes mainly included those related to the SA pathway, such as late blight-resistant genes (*R1* genes such as RIB-08, 16, 17, and RPP 8, 13), *PR* genes (*PR4*, including defensin-like protein 1), JA/ET-related *ERF* genes, and other defense-related genes (STH-2

and MLO-like 6). Expression heatmap (TPM) showed a higher ratio of these upregulated defense genes in the KGMOS-treated group compared to the control (Figure 5A). Further analysis of *PR* and *NPR* genes more clearly indicated that SA pathway-related genes (*PR1*, *PR2*, *PR4*, *PR5*, *PR14*, *NPR1*, and *NPR3*) were involved in a different ratio in the KGMOS group compared to the control after pathogen infection (Figure 5B,C and Supplementary Table S5). These overall results suggest that KGMOS triggered the SA and JA/ET signaling pathways, enhancing disease resistance against *P. nicotianae* inoculation.

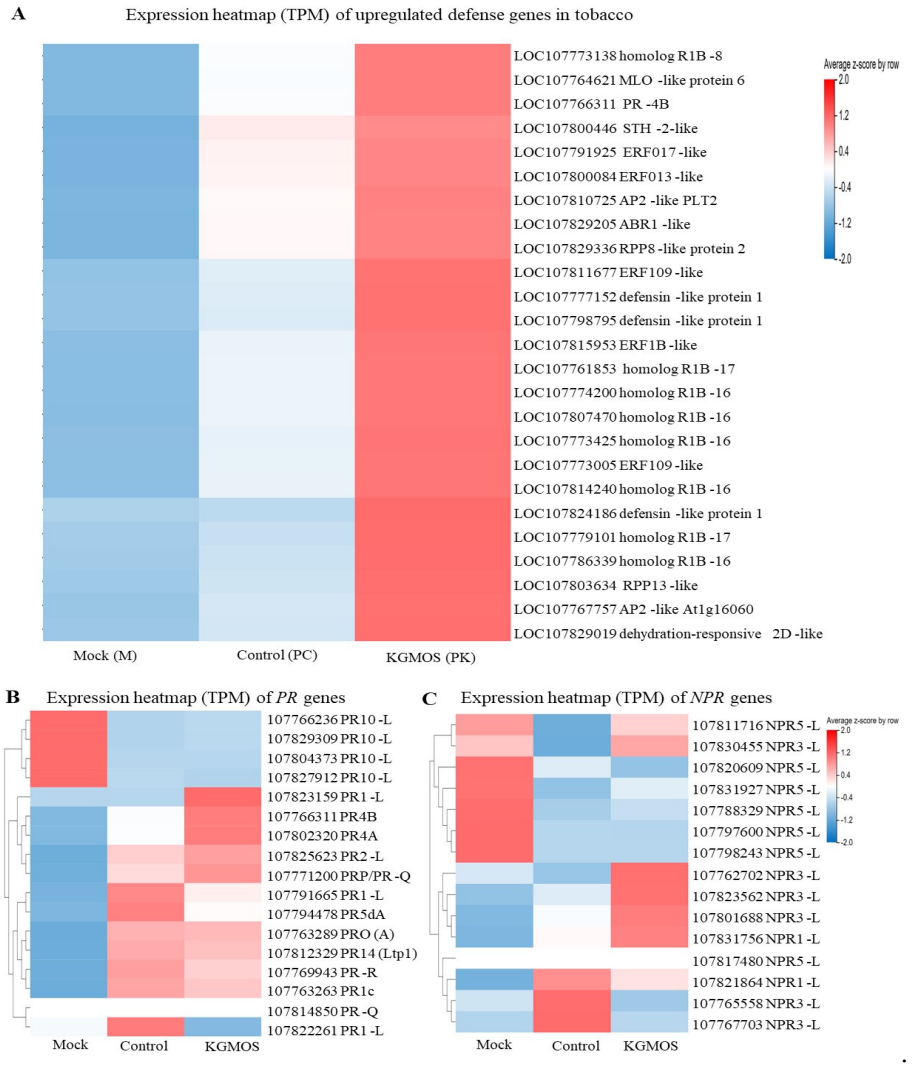

Figure 5. Heatmap analysis of defense genes among mock, control (PC), and KGMOS groups (PK). (**A**) The expression of upregulated defense genes in the KGMOS group compared to control and mock. (**B**) The expression of *PR* genes among mock, control, and KGMOS groups. (**C**) The expression of SA signaling pathway-related genes among mock, control, and KGMOS groups. TPM = transcripts per kilobase million.

Upregulated DEGs in KGMOS-treated plants showed significant involvement in key resistance pathways, including oxidative phosphorylation, plant–pathogen interaction, phenylpropanoid biosynthesis, MAPK signaling, biosynthesis of amino acids, and carbon metabolism. The GO annotation highlighted protein phosphorylation and other defense-related pathways, confirming the activation of MAPK signaling, plant–pathogen interaction, and plant hormone signal transduction. The higher involvement of genes related to peroxidase enzymes, calcium-dependent protein kinase, and MAPK-related genes in the KGMOS group compared to the control group suggests increased H_2O_2 production, callose deposition, lignification, and activation of SA and JA/ET pathways. Further analysis

revealed the upregulation of defense genes related to the SA pathway, including R and PR genes and JA/ET-related ERF genes, in the KGMOS group. Overall, KGMOS treatment triggers PTI and ETI-related signaling molecules, proteins, and genes associated with the SA and JA/ET pathways, enhancing disease resistance against *P. nicotianae*.

3.4. KGMOS Activated SA and JA/ET Pathway in Tobacco

To confirm the transcriptomic data, the expression of genes related to the SA and JA/ET pathways was selected for assessment by using RT-qPCR. Compared with control, KGMOS pre-treated (25 mg/L) plants displayed a comparable pattern (Figure 6A), showing a 3.36-, 9.28-, 5.41-, 2.31-, 2.69-, 4.36-, and 8.67-fold change for *NPR1*, *PR1a*, *PR2*, *PR4*, *PR5* (thaumatin), *PR12* (defensin), and JA/ET pathway genes of *ERF1* (*ETHYLENE RESPONSE FACTOR1*), respectively. To validate these findings, the content of SA was also confirmed by LC–MS analysis. The content of SA in KGMOS groups (25–100 mg/L) was higher than in control groups, but only the 25 mg/L concentration showed a significant difference compared to the control group (Figure 6B). The content of SA in the 25 mg/L KGMOS group (1508.89 ng/g) was 2.62-fold higher than the control group (575.63 ng/g), suggesting that KGMOS might enhance disease resistance by augmenting SA accumulation. These data suggest that the SA and JA/ET signaling pathways are activated following *P. nicotianae* inoculation after being pre-treated with KGMOS in plants.

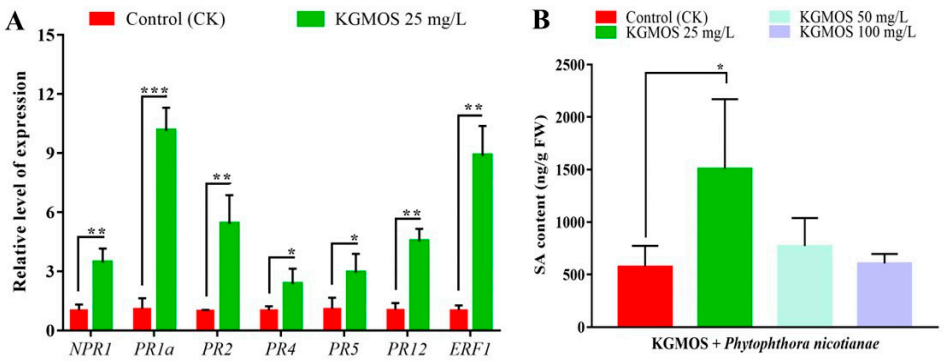

Figure 6. KGMOS induced SA and JA/ET pathway in *N. benthamiana*. (**A**) The relative expression of SA pathway genes detected by RT-qPCR. The control (CK) was normalized as 1. (**B**) The content of SA in infected leaves pre-treated with KGMOS. SPSS (version 22) was used to analyze data, and means were compared with the LSD at 0.05. Values are presented as the means ± SD of three independent measurements. Asterisks indicate significant differences (* $p < 0.05$, ** $p < 0.01$, *** $p < 0.001$).

This study contributes to a better understanding of how KGMOS activates plant immunity, enabling researchers to design more effective strategies for boosting plant defenses in agricultural settings. The dual activation of PTI and ETI underscores the potential of KGMOS as a broad-spectrum elicitor capable of conferring resistance to a wide range of fungi, bacteria, and viruses. Notably, KGMOS triggers both SA- and JA/ET-mediated defenses, suggesting its utility in protecting plants against biotrophs (SAR) and necrotrophs (ISR), respectively. This versatility sets KGMOS apart from many conventional elicitors, which typically activate only one of these pathways (SA, JA, or ET). Moreover, integrating water-soluble biodegradable KGMOS into integrated pest management (IPM) strategies could reduce reliance on chemical pesticides, promoting sustainable agriculture.

4. Discussion

Storage polysaccharide-derived oligosaccharides have recently gained global attention due to their eco-friendly nature [46,47]. Research has shown that oligosaccharides such as AOS (Alginate oligosaccharides), FOS, and MOS are effective against various plant pathogens. However, the mechanisms by which mannose-enriched derived oligosaccharides (KGMOS) confer plant defense responses are yet to be elucidated. In this study, we

investigated KGMOS-mediated resistance to *P. nicotianae* in *N. benthamiana* at the phenotypic and molecular levels. Our study demonstrated that KGMOS could induce defense responses against the black shank pathogen in tobacco plants. These responses include decelerated mycelial growth, decreased disease index, an increase in H_2O_2 accumulation and callose deposition in infected leaves, and upregulation of defense-related genes through activating SA and JA/ET signaling pathways.

KGMOS exhibited antifungal activity and reduced necrosis symptoms against the black shank pathogen in tobacco. When treating *P. nicotianae* in vivo and in situ with different concentrations of KGMOS, we found that the lower concentration (25 mg/L) was the most effective in inhibiting pathogen proliferation. However, increased concentrations of KGMOS resulted in a reduction in inhibition activity. A similar trend was observed for H_2O_2 accumulation and callose deposition in leaves, with lower concentrations of KGMOS activating higher levels of signaling molecules. ROS accumulation and release are the earliest events in plant–pathogen interactions [48–50]. Callose deposition, mediated by SA as reported in *Arabidopsis* [51], slowed down filamentous pathogen invasion and spread during biotic stress [52,53]. Several oligosaccharides derived from storage polysaccharides such as AOS, FOS, and MOS are also capable of eliciting ROS accumulation in epidermal cells and reducing pathogen invasion in *Arabidopsis* [54], rice, and tobacco [35,55]. Additionally, it has been reported that KGMOS also inhibited the fungal proliferation of *Candida albicans* [36] and diseases caused by *Aeromonas hydrophila* in Nile tilapia fish [39], which supports the present study.

In our study, we analyzed the DEGs in the transcriptome of KGMOS-pre-treated and untreated *N. benthamiana* after pathogen infection compared to non-infected mock plants. Meanwhile, an increased number of upregulated DEGs in the KGMOS group (420) than in the control group was identified after pathogen infections. These upregulated DEGs from both groups were associated with various resistance pathways, such as MAPK signaling, plant–pathogen interaction, plant hormone signal transduction, and phenylpropanoid biosynthesis, which ultimately trigger and activate the SA and JA/ET signaling pathways. The DEGs from the KGMOS-treated group were more involved in these pathways compared to the control. KEGG and GO annotation of distinct and overlapped genes in KGMOS and control groups also revealed their correlation with resistance-related hydrogen peroxide signaling and phenylpropanoid biosynthesis, including SA and JA/ET signaling pathways. Thus, some genes associated with these pathways were selected as immune response indicators to confirm the quality of our transcriptome data. Our RT-qPCR data demonstrated that these defense response genes were significantly upregulated in KGMOS-treated *N. benthamiana* plants compared to the control group post-inoculation with *P. nicotianae*. Previous studies have reported that the expression of SA and JA/ET-related genes was induced after *P. nicotianae* infection, which also supports our conclusion that KGMOS-regulated disease resistance to *P. nicotianae* is mediated by SA and JA/ET signaling pathways [56,57].

Multiple phytohormones regulate plant resistance to pathogen attack, including SA, JA, and ET [58,59]. SA, as well as JA/ET signaling pathways, play crucial roles in necrotrophic and hemi-biotrophic pathogens [60,61]. Both the SA and JA/ET pathways play a role in modulating resistance to the *P. nicotianae* pathogen [56]. SA affects the transcription of the long-term defense marker *PR1* [62], a key player in SA-induced immune pathways and SAR monitoring [63,64]. The PR1 proteins from tomato and tobacco have been proven to directly prevent the germination of zoospores with *P. infestans* in vitro [65]. Overexpression of PR1 in *Arabidopsis* triggers the recruitment of additional PR proteins, such as PR2, PR3, PR4, PR5, and PR14 [66]. These PR proteins could directly affect pathogen integrity through their efficacy [67] and/or trigger signaling molecules (ROS) generation to defend against divergent pathogens in *Arabidopsis*, tobacco, and wheat [27,68,69]. This study focuses on KGMOS pre-treatment-mediated disease resistance against *P. nicotianae*, unraveling the intricate mechanisms underlying SA and JA/ET signaling pathways. Compared to the control group, tobacco plants treated with KGMOS (25 mg/L) showed significant SA

accumulation, which activates *NPR1* and induces upregulation of *PR* genes (*PR1a*, *PR2*, *PR4*, *PR5*, and *PR12*). The expression level of key genes in the JA/ET pathway, such as *ERF1*, was also upregulated in response to the same KGMOS treatment. The upregulation of DEGs in the KGMOS group related to various resistance pathways suggests that KGMOS may function as an elicitor. Previous research has established that CERK1 (Chitin Elicitor Receptor Kinase 1) serves as the receptor for chitosan oligosaccharides (COS), a well-characterized oligosaccharide elicitor [70]. Additionally, WAK1 (Wall-associated Kinase 1) has been identified as the receptor for oligogalacturonic acids (OGA), which are products of pectin degradation [71]. Both COS and OGA are known to act as elicitors, triggering downstream defense responses such as the MAPK (Mitogen-Activated Protein Kinase) pathway and hormone signaling pathways. Moreover, flg22 acts as an elicitor recognized by the FLS2 (FLAGELLIN SENSING 2) receptor and the co-receptor BAK1 (BRI1-ASSOCIATED RECEPTOR KINASE 1) [72]. These receptors, co-receptors, and associated proteins mediate the activation of WRKY22/29, leading to H_2O_2 accumulation and the induction of SA-related defense genes like *PR1* and *NPR1* [4]. Transcriptome analysis indicates that the CERK1 receptor, BAK1 co-receptor, mitogen-activated protein kinase 3-like, mitogen-activated protein kinase homolog MMK2-like, WRKY29, *PR*s, and *NPR1* are involved in the KGMOS response. Additionally, various calcium-dependent protein kinases (CDPKs) were upregulated in the KGMOS group, suggesting their role in regulating ROS production, callose deposition, cell wall reinforcement, and defense responses. We speculate that KGMOS may act in a manner similar to other elicitors, such as COS and OGA. However, further research is needed to confirm the involvement of specific receptors and co-receptors in the KGMOS response. FOS has been reported to induce resistance by modulating ROS, *PR* genes, and the SA pathway [34]. However, the majority of FOS research has been focused on specific crops and pathogens, with an emphasis primarily on managing postharvest diseases. This demonstrates that storage polysaccharide-derived oligosaccharides can trigger plant immunity by activating downstream signaling molecules. Our study is further supported by findings on AOS and MOS, which have also demonstrated resistance against various pathogens through the SA and JA/ET pathways, as well as by inducing the expression of related genes [35,73]. Therefore, KGMOS has a high probability of contributing to sustainable agricultural practices both in the field and in postharvest storage.

Although this study provides valuable insights into the mechanisms of KGMOS-induced plant immunity and its potential to combat a wide range of pathogens by inducing both SA and JA/ET pathways, several limitations should be acknowledged. This study primarily focused on tobacco plants challenged with the pathogen *P. nicotianae* under laboratory conditions. The efficacy of KGMOS needs to be tested across various crops and field conditions, considering diverse environmental stresses, microbes, and insects. Additionally, the long-term effects of KGMOS treatment on plant morpho-physiology, yield, and soil health were not addressed. Testing KGMOS against a variety of biotic and abiotic factors across different plant species under natural conditions will help establish its broad-spectrum potential. Furthermore, assessing KGMOS's impact on plant, soil, and environmental health is essential for confirming its safety. KGMOS has the potential to reduce reliance on chemical pesticides in the field, fresh preservation, and postharvest management, promoting more sustainable and environmentally friendly agricultural practices and safe food production. Integrating KGMOS into integrated pest management (IPM) strategies, complementing other biological control agents and cultural practices, can enhance the effectiveness of plant disease management.

5. Conclusions

KGMOS is gaining appeal as a natural elicitor due to its cost-effectiveness and physicochemical properties for enhancing plant immunity, food safety, and soil health. This study identified the resistance attributes of KGMOS against *P. nicotianae* in *N. benthamiana* using physiological experiments and a transcriptome-sequencing approach. The inhibitory

effect extends beyond antifungal activity, encompassing their capacity to induce defense molecules, pathogen resistance genes, transcription factor genes, and SA and JA/ET signaling genes. In particular, we observed a higher activity with a lower concentration of KGMOS (25 mg/L). This treatment activates key resistance pathways, including peroxidase enzymes, calcium-dependent protein kinase, and MAPK, leading to increased H_2O_2 production, callose deposition, and lignification associated with PTI. Additionally, it upregulates ETI-related SA and JA/ET pathway genes. These findings indicate that KGMOS effectively triggers PTI and ETI-related signaling molecules and genes to enhance disease resistance against *P. nicotianae*. Subsequent research will pay attention to addressing essential questions, including whether KGMOS directly targets proteins or genes in tobacco or the pathogen or whether they interfere with the interaction between them. Field trials with diverse biotic and abiotic stressors are also suggested to prove the broad-spectrum potential of KGMOS. The findings of this study offer valuable insights into the immunomodulatory roles of KGMOS and its potential applications in crop protection and postharvest for sustainable agriculture and integrated pest management strategies.

Supplementary Materials: The following supporting information can be downloaded at: https://www.mdpi.com/article/10.3390/agriculture14081289/s1, Figure S1: The H_2O_2 and callose deposition in *N. benthamiana* under control and KGMOS treatments; Figure S2: Upregulated phosphorylation related and downregulated DEGs from *N. benthamiana* at 3 days after *P. nicotianae* infection; Figure S3: Involvement of genes after *P. nicotianae* infection in *N. benthamiana* among mock, control (PC), and KGMOS (PK) groups; Table S1: List of primers used for q-PCR; Table S2: Disease index, fungal growth, and inhibition by different treatments; Table S3: Overlap upregulated DEGs related to phosphorylation in between KGMOS (PK)/mock and control (PC)/mock; Table S4: Overlapped defense responsive genes upregulated in KGMOS (PK) compare to control (PC) and Mock (M); Table S5: Expression of *PR* (*PATHOGENESIS-RELATED*) and *NPR* (*NONEXPRESSOR OF PR*) genes in between control (PC), and KGMOS (PK) group.

Author Contributions: M.M.R.R.: conceptualization, methodology, software, validation, formal analysis, investigation, writing—original draft preparation, and visualization; K.L.: resources, validation, writing—review and editing, and visualization; M.S.H.B.: formal analysis, investigation, visualization, and writing—review and editing; W.W.: investigation, resource, supervision, and writing—review and editing; J.G.: validation, writing—review and editing, and visualization; H.Y.: validation, resources, data curation, supervision, project administration, and funding acquisition. All authors have read and agreed to the published version of the manuscript.

Funding: This work was supported by the National Key Research and Development Project of China (2023YFD1700600), the National Natural Science Foundation of China (32270210, 32000905), the Dalian Institute of Chemical Physics Innovation Research Fund Project (DICP I202412), the ANSO Collaborative Research Program (ANSO-CR-KP-2020-14), and the Sichuan Provincial Regional Cooperation Innovation Project (24QYCX0072).

Data Availability Statement: The data supporting the findings of this study will be available upon reasonable request.

Acknowledgments: Md. Mijanur Rahman Rajib was supported by DICP and the CAS PhD program, and he is very grateful to DICP and UCAS.

Conflicts of Interest: The authors affirm that there are no conflicts of interest associated with this publication. Their research in this manuscript is not influenced by any financial, personal, or professional relationships. We ensured the integrity and impartiality of the study by generating and analyzing all data independently.

References

1. Bhandari, D.D.; Ko, D.K.; Kim, S.-J.; Nomura, K.; He, S.Y.; Brandizzi, F. Defense against phytopathogens relies on efficient antimicrobial protein secretion mediated by the microtubule-binding protein TGNap1. *Nat. Commun.* **2023**, *14*, 6357. [CrossRef] [PubMed]
2. Ngou, B.P.M.; Ahn, H.-K.; Ding, P.; Jones, J.D.G. Mutual potentiation of plant immunity by cell-surface and intracellular receptors. *Nature* **2021**, *592*, 110–115. [CrossRef]

3. Ngou, B.P.M.; Ding, P.; Jones, J.D.G. Thirty years of resistance: Zig-zag through the plant immune system. *Plant Cell* **2022**, *34*, 1447–1478. [CrossRef] [PubMed]
4. Yuan, M.; Jiang, Z.; Bi, G.; Nomura, K.; Liu, M.; Wang, Y.; Cai, B.; Zhou, J.-M.; He, S.Y.; Xin, X.-F. Pattern-recognition receptors are required for NLR-mediated plant immunity. *Nature* **2021**, *592*, 105–109. [CrossRef]
5. Jones, J.D.G.; Dangl, J.L. The plant immune system. *Nature* **2006**, *444*, 323–329. [CrossRef]
6. Pruitt, R.N.; Gust, A.A.; Nürnberger, T. Plant immunity unified. *Nat. Plants* **2021**, *7*, 382–383. [CrossRef]
7. Minhang, Y.; Bruno Pok Man, N.; Pingtao, D.; Xiu-Fang, X. PTI-ETI crosstalk: An integrative view of plant immunity. *Curr. Opin. Plant Biol.* **2021**, *62*, 102030. [CrossRef]
8. Peng, Y.; van Wersch, R.; Zhang, Y. Convergent and Divergent Signaling in PAMP-Triggered Immunity and Effector-Triggered Immunity. *Mol. Plant-Microbe Interact. MPMI* **2018**, *31*, 403–409. [CrossRef] [PubMed]
9. Thulasi Devendrakumar, K.; Li, X.; Zhang, Y. MAP kinase signalling: Interplays between plant PAMP- and effector-triggered immunity. *Cell. Mol. Life Sci.* **2018**, *75*, 2981–2989. [CrossRef]
10. Zhou, J.M.; Zhang, Y. Plant Immunity: Danger Perception and Signaling. *Cell* **2020**, *181*, 978–989. [CrossRef]
11. Liu, L.; Sonbol, F.M.; Huot, B.; Gu, Y.; Withers, J.; Mwimba, M.; Yao, J.; He, S.Y.; Dong, X. Salicylic acid receptors activate jasmonic acid signalling through a non-canonical pathway to promote effector-triggered immunity. *Nat. Commun.* **2016**, *7*, 13099. [CrossRef] [PubMed]
12. Vlot, A.C.; Sales, J.H.; Lenk, M.; Bauer, K.; Brambilla, A.; Sommer, A.; Chen, Y.; Wenig, M.; Nayem, S. Systemic propagation of immunity in plants. *J. New Phytol.* **2021**, *229*, 1234–1250. [CrossRef] [PubMed]
13. Nie, P.; Li, X.; Wang, S.; Guo, J.; Zhao, H.; Niu, D. Induced systemic resistance against Botrytis cinerea by *Bacillus cereus* AR156 through a JA/ET-and NPR1-dependent signaling pathway and activates PAMP-triggered immunity in *Arabidopsis*. *J. Front. Plant Sci.* **2017**, *8*, 247629. [CrossRef] [PubMed]
14. Boccardo, N.A.; Segretin, M.E.; Hernandez, I.; Mirkin, F.G.; Chacón, O.; Lopez, Y.; Borrás-Hidalgo, O.; Bravo-Almonacid, F.F. Expression of pathogenesis-related proteins in transplastomic tobacco plants confers resistance to filamentous pathogens under field trials. *Sci. Rep.* **2019**, *9*, 2791. [CrossRef] [PubMed]
15. Hong, Y.; Zheng, Q.; Cheng, L.; Liu, P.; Xu, G.; Zhang, H.; Cao, P.; Zhou, H. Identification and characterization of TMV-induced volatile signals in *Nicotiana benthamiana: Evidence* for JA/ET defense pathway priming in congeneric neighbors via airborne (E)-2-octenal. *J. Funct. Integr. Genom.* **2023**, *23*, 272. [CrossRef] [PubMed]
16. Kroon, L.P.; Brouwer, H.; de Cock, A.W.; Govers, F. The genus *Phytophthora* anno 2012. *Phytopathology* **2012**, *102*, 348–364. [CrossRef] [PubMed]
17. Wang, W.; Jiao, F. Effectors of *Phytophthora* pathogens are powerful weapons for manipulating host immunity. *Planta* **2019**, *250*, 413–425. [CrossRef] [PubMed]
18. Chen, X.; He, B.; Yang, H.; Cernava, T. Bacteriome and Mycobiome in *Nicotiana tabacum* Fields Affected by Black Shank Disease. *Plant Dis.* **2020**, *104*, 315–319. [CrossRef] [PubMed]
19. Gallup, C.A.; McCorkle, K.L.; Ivors, K.L.; Shew, D. Characterization of the Black Shank Pathogen, *Phytophthora nicotianae*, Across North Carolina Tobacco Production Areas. *Plant Dis.* **2018**, *102*, 1108–1114. [CrossRef]
20. Meng, Y.; Zhang, Q.; Ding, W.; Shan, W. *Phytophthora parasitica*: A model oomycete plant pathogen. *Mycology* **2014**, *5*, 43–51. [CrossRef]
21. Hou, Y.; Zhai, Y.; Feng, L.; Karimi, H.Z.; Rutter, B.D.; Zeng, L.; Choi, D.S.; Zhang, B.; Gu, W.; Chen, X.; et al. A *Phytophthora* Effector Suppresses Trans-Kingdom RNAi to Promote Disease Susceptibility. *Cell Host Microbe* **2019**, *25*, 153–165.e155. [CrossRef] [PubMed]
22. Lee, J.H.; Lee, S.E.; Oh, S.; Seo, E.; Choi, D. HSP70s Enhance a *Phytophthora infestans* Effector-Induced Cell Death via an MAPK Cascade in *Nicotiana benthamiana*. *Mol. Plant-Microbe Interact. MPMI* **2018**, *31*, 356–362. [CrossRef] [PubMed]
23. Yang, B.; Yang, S.; Zheng, W.; Wang, Y. Plant immunity inducers: From discovery to agricultural application. *Stress Biol.* **2022**, *2*, 5. [CrossRef] [PubMed]
24. Boutrot, F.; Zipfel, C. Function, Discovery, and Exploitation of Plant Pattern Recognition Receptors for Broad-Spectrum Disease Resistance. *Annu. Rev. Phytopathol.* **2017**, *55*, 257–286. [CrossRef] [PubMed]
25. Hao, W.; Gray, M.A.; Förster, H.; Adaskaveg, J.E. Evaluation of New Oomycota Fungicides for Management of *Phytophthora* Root Rot of Citrus in California. *Plant Dis.* **2019**, *103*, 619–628. [CrossRef] [PubMed]
26. Wang, Y.; Tyler, B.M.; Wang, Y. Defense and Counterdefense During Plant-Pathogenic Oomycete Infection. *Annu. Rev. Microbiol.* **2019**, *73*, 667–696. [CrossRef] [PubMed]
27. Sun, M.; Li, L.; Wang, C.; Wang, L.; Lu, D.; Shen, D.; Wang, J.; Jiang, C.; Cheng, L.; Pan, X.; et al. Naringenin confers defence against *Phytophthora nicotianae* through antimicrobial activity and induction of pathogen resistance in tobacco. *Mol. Plant Pathol.* **2022**, *23*, 1737–1750. [CrossRef] [PubMed]
28. Zhang, P.Y.; Wang, J.C.; Liu, S.H.; Chen, K.S. A novel burdock fructooligosaccharide induces changes in the production of salicylates, activates defence enzymes and induces systemic acquired resistance to *Colletotrichum orbiculare* in cucumber seedlings. *J. Phytopathol.* **2009**, *157*, 201–207. [CrossRef]
29. Hao LinHua, H.L.; Chen KaoShan, C.K.; Li GuangYou, L.G. Physiological effects of Burdock oligosaccharide on growth promotion and chilling resistance of cucumber seedlings. *J. Shanghai Jiaotong Univ.—Agric. Sci.* **2006**, *24*, 6–12.

30. He, P.Q.; Tian, L.; Chen, K.S.; Hao, L.H.; Li, G.Y. Induction of volatile organic compounds of *Lycopersicon esculentum* Mill. and its resistance to *Botrytis cinerea* Pers. by burdock oligosaccharide. *J. Integr. Plant Biol.* **2006**, *48*, 550–557. [CrossRef]
31. Wang, F.; Feng, G.; Chen, K. Defense responses of harvested tomato fruit to burdock fructooligosaccharide, a novel potential elicitor. *J. Postharvest Biol.* **2009**, *52*, 110–116. [CrossRef]
32. Sun, F.; Zhang, P.; Guo, M.; Yu, W.; Chen, K. Burdock fructooligosaccharide induces fungal resistance in postharvest Kyoho grapes by activating the salicylic acid-dependent pathway and inhibiting browning. *J. Food Chem.* **2013**, *138*, 539–546. [CrossRef] [PubMed]
33. Zhang, H.; Liu, Z.; Xu, B.; Chen, K.; Yang, Q.; Zhang, Q. Burdock fructooligosaccharide enhances biocontrol of *Rhodotorula mucilaginosa* to postharvest decay of peaches. *Carbohydr. Polym.* **2013**, *98*, 366–371. [CrossRef] [PubMed]
34. Guo, M.; Chen, G.; Chen, K. *Fructooligosaccharides: Effects, mechanisms, and applications. Research Progress in Oligosaccharins*; Springer: New York, NY, USA, 2016; pp. 51–63. [CrossRef]
35. Zang, H.; Xie, S.; Zhu, B.; Yang, X.; Gu, C.; Hu, B.; Gao, T.; Chen, Y.; Gao, X. Mannan oligosaccharides trigger multiple defence responses in rice and tobacco as a novel danger-associated molecular pattern. *Mol. Plant Pathol.* **2019**, *20*, 1067–1079. [CrossRef]
36. Tester, R.; Al-Ghazzewi, F.H. Role of glucomannans in immunology. *J. Pharm. Pharm. Sci.* **2017**, *20*, 97–114. [CrossRef] [PubMed]
37. Faustino, M.; Durão, J.; Pereira, C.F.; Pintado, M.E.; Carvalho, A.P. Mannans and mannan oligosaccharides (MOS) from *Saccharomyces cerevisiae*—A sustainable source of functional ingredients. *Carbohydr. Polym.* **2021**, *272*, 118467. [CrossRef]
38. Zhang, Y.; Zhao, Y.; Yang, W.; Song, G.; Zhong, P.; Ren, Y.; Zhong, G. Structural complexity of Konjac glucomannan and its derivatives governs the diversity and outputs of gut microbiota. *Carbohydr. Polym.* **2022**, *292*, 119639. [CrossRef]
39. Zheng, Q.; Wu, Y.; Xu, H.; Wang, H.; Tang, H.; Xia, X.; Feng, J. Immune responses to *Aeromonas hydrophila* infection in Schizothorax prenanti fed with oxidized konjac glucomannan and its acidolysis products. *Fish Shellfish Immunol.* **2016**, *49*, 260–267. [CrossRef]
40. Chen, L.; Zhang, S.; Wu, S.; Ren, Z.; Liu, G.; Wu, J. Synergistic Protective Effect of Konjac Mannan Oligosaccharides and *Bacillus subtilis* on Intestinal Epithelial Barrier Dysfunction in Caco-2 Cell Model and Mice Model of Lipopolysaccharide Stimulation. *Front. Immunol.* **2021**, *12*, 696148. [CrossRef]
41. Tang, J.; Liu, J.; Yan, Q.; Gu, Z.; August, A.; Huang, W.; Jiang, Z. Konjac Glucomannan Oligosaccharides Prevent Intestinal Inflammation Through SIGNR1-Mediated Regulation of Alternatively Activated Macrophages. *Mol. Nutr. Food Res.* **2021**, *65*, e2001010. [CrossRef]
42. Gao, J.; Huang, G.; Chen, X.; Zhu, Y.X. PROTEIN S-ACYL TRANSFERASE 13/16 modulate disease resistance by S-acylation of the nucleotide binding, leucine-rich repeat protein R5L1 in Arabidopsis. *J. Integr. Plant Biol.* **2022**, *64*, 1789–1802. [CrossRef] [PubMed]
43. Schenk, S.T.; Schikora, A. Staining of Callose Depositions in Root and Leaf Tissues. *Bio-protocol* **2015**, *5*, e1429. [CrossRef]
44. Livak, K.J.; Schmittgen, T.D. Analysis of relative gene expression data using real-time quantitative PCR and the 2(-Delta Delta C(T)) Method. *Methods* **2001**, *25*, 402–408. [CrossRef] [PubMed]
45. Pan, X.; Welti, R.; Wang, X. Quantitative analysis of major plant hormones in crude plant extracts by high-performance liquid chromatography-mass spectrometry. *Nat. Protoc.* **2010**, *5*, 986–992. [CrossRef] [PubMed]
46. Tester, R.; Al-Ghazzewi, F. Glucomannans and nutrition. *Food Hydrocoll.* **2017**, *68*, 246–254. [CrossRef]
47. Akesowan, A. Optimization of Textural Properties of Konjac Gels Formed with κ-Carrageenan or Xanthan and Xylitol as Ingredients in Jelly Drink Processing. *J. Food Process. Preserv.* **2015**, *39*, 1735–1743. [CrossRef]
48. Sayanti, M.; Sivasubramanian, R.; Jagreet, K. ROS accumulation and associated cell death mediates susceptibility to *Alternaria brassicae* in *Arabidopsis* accessions. *Physiol. Mol. Plant Pathol.* **2019**, *107*, 51–59. [CrossRef]
49. Mejía-Teniente, L.; Durán-Flores, B.A.; Torres-Pacheco, I.; González-Chavira, M.M.; Rivera-Bustamante, R.F.; Feregrino-Pérez, A.A.; Pérez-Ramírez, I.F.; Rocha-Guzmán, N.E.; Reynoso-Camacho, R.; Guevara-González, R.G. Hydrogen peroxide protects pepper (Capsicum annuum L.) against pepper golden mosaic geminivirus (PepGMV) infections. *Physiol. Mol. Plant Pathol.* **2019**, *106*, 23–29. [CrossRef]
50. Daymi, C.; Ángel, G.-C.; Alexander, M. Reactive oxygen species, essential molecules, during plant–pathogen interactions. *Plant Physiol. Biochem.* **2016**, *103*, 10–23. [CrossRef]
51. Wang, X.; Sager, R.; Cui, W.; Zhang, C.; Lu, H.; Lee, J.-Y. Salicylic Acid Regulates Plasmodesmata Closure during Innate Immune Responses in *Arabidopsis*. *Plant Cell* **2013**, *25*, 2315–2329. [CrossRef]
52. Wang, Y.; Li, X.; Fan, B.; Zhu, C.; Chen, Z. Regulation and Function of Defense-Related Callose Deposition in Plants. *Int. J. Mol. Sci.* **2021**, *22*, 2393. [CrossRef] [PubMed]
53. Wang, B.; Andargie, M.; Fang, R. The function and biosynthesis of callose in high plants. *Heliyon* **2022**, *8*, e09248. [CrossRef]
54. Zhang, C.; Howlader, P.; Liu, T.; Sun, X.; Jia, X.; Zhao, X.; Shen, P.; Qin, Y.; Wang, W.; Yin, H. Alginate Oligosaccharide (AOS) induced resistance to *Pst* DC3000 via salicylic acid-mediated signaling pathway in *Arabidopsis thaliana*. *Carbohydr. Polym.* **2019**, *225*, 115221. [CrossRef] [PubMed]
55. Guo, M.; Chen, K. *Transcriptome Profile Analysis and Signal Transduction of Resistance Induced by Burdock Fructooligosaccharide in Tobacco*; Shandong University: Jinan, China, 2014.
56. Liming, W.; Ziyang, H.; Xi, L.; Liumin, M.; Qin, G.; Huijun, W.; Jia, L.; Rainer, B.; Zhen, W.; Xuewen, G. Stomatal closure and SA-, JA/ET-signaling pathways are essential for Bacillus amyloliquefaciens FZB42 to restrict leaf disease caused by *Phytophthora nicotianae* in *Nicotiana benthamiana*. *Front. Microbiol.* **2018**, *9*, 847. [CrossRef]

57. Wang, W.; Zhang, J.; Cao, Y.; Yang, X.; Wang, F.; Yang, J.; Wang, X. NtbHLH49, a jasmonate-regulated transcription factor, negatively regulates tobacco responses to *Phytophthora nicotianae*. *Front. Plant Sci.* **2022**, *13*, 1073856. [CrossRef] [PubMed]
58. Mishra, B.; Bose, S.K.; Sangwan, N.S. Comparative investigation of therapeutic plant Withania somnifera for yield, productivity, withanolide content, and expression of pathway genes during contrasting seasons. *Ind. Crops Prod.* **2020**, *154*, 112508. [CrossRef]
59. Li, W.; Zhao, D.; Dong, J.; Kong, X.; Zhang, Q.; Li, T.; Meng, Y.; Shan, W. AtRTP5 negatively regulates plant resistance to *Phytophthora* pathogens by modulating the biosynthesis of endogenous jasmonic acid and salicylic acid. *Mol. Plant Pathol.* **2020**, *21*, 95–108. [CrossRef]
60. Robert-Seilaniantz, A.; Grant, M.; Jones, J.D. Hormone crosstalk in plant disease and defense: More than just jasmonate-salicylate antagonism. *Annu. Rev. Phytopathol.* **2011**, *49*, 317–343. [CrossRef]
61. Howlader, P.; Bose, S.K.; Jia, X.; Zhang, C.; Wang, W.; Yin, H. Oligogalacturonides induce resistance in *Arabidopsis thaliana* by triggering salicylic acid and jasmonic acid pathways against *Pst* DC3000. *Int. J. Biol. Macromol.* **2020**, *164*, 4054–4064. [CrossRef]
62. Loon, L.C.v.; Rep, M.; Pieterse, C.M.J. Significance of Inducible Defense-related Proteins in Infected Plants. *Annu. Rev. Phytopathol.* **2006**, *44*, 135–162. [CrossRef]
63. Susan, B.; Simon, J.W.; Megan, O.; Bostjan, K.; Peter, S.S. Emerging Insights into the Functions of Pathogenesis-Related Protein 1. *Trends Plant Sci.* **2017**, *22*, 871–879. [CrossRef]
64. Vlot, A.C.; Dempsey, D.A.; Klessig, D.F. Salicylic Acid, a multifaceted hormone to combat disease. *Annu. Rev. Phytopathol.* **2009**, *47*, 177–206. [CrossRef] [PubMed]
65. Niderman, T.; Genetet, I.; Bruyere, T.; Gees, R.; Stintzi, A.; Legrand, M.; Fritig, B.; Mosinger, E. Pathogenesis-Related PR-1 Proteins Are Antifungal (Isolation and Characterization of Three 14-Kilodalton Proteins of Tomato and of a Basic PR-1 of Tobacco with Inhibitory Activity against *Phytophthora infestans*). *Plant Physiol.* **1995**, *108*, 17–27. [CrossRef] [PubMed]
66. Han, Z.; Xiong, D.; Schneiter, R.; Tian, C. The function of plant PR1 and other members of the CAP protein superfamily in plant–pathogen interactions. *Mol. Plant Pathol.* **2023**, *24*, 651–668. [CrossRef] [PubMed]
67. Edreva, A. Pathogenesis-related proteins: Research progress in the last 15 years. *Gen. Appl. Plant Physiol.* **2005**, *31*, 105–124.
68. Yang, L.; Gangliang, H.; Meijiao, L. Extraction, characterization and antioxidant activities of mannan from yeast cell wall. *Int. J. Biol. Macromol.* **2018**, *118*, 952–956. [CrossRef]
69. Xiumei, L.; Tingting, T.; Li, F.; Xingyong, Y.; Linxuan, L.; Xue, T.; Wenxian, W.; Zhengguo, L.; Haim, T.; Francois, S.; et al. Pathogenesis-related protein 1 suppresses oomycete pathogen by targeting against AMPK kinase complex. *J. Adv. Res.* **2023**, *43*, 13–26. [CrossRef]
70. Yang, C.; Wang, E.; Liu, J. CERK1, more than a co-receptor in plant–microbe interactions. *New Phytol.* **2022**, *234*, 1606–1613. [CrossRef] [PubMed]
71. Ferrari, S.; Savatin, D.V.; Sicilia, F.; Gramegna, G.; Cervone, F.; Lorenzo, G.D. Oligogalacturonides: Plant damage-associated molecular patterns and regulators of growth and development. *Front. Plant Sci.* **2013**, *4*, 49. [CrossRef]
72. Zhao, Q.; Bao, J.; Li, H.; Hu, W.; Kong, Y.; Zhong, Y.; Fu, Q.; Xu, G.-y.; Liu, F.; Jia, X.; et al. Structural and biochemical basis of FLS2-mediated signal activation and transduction in rice. *Plant Commun.* **2024**, *5*, 100785. [CrossRef]
73. Zhang, C.; Wang, W.; Zhao, X.; Wang, H.; Yin, H. Preparation of alginate oligosaccharides and their biological activities in plants: A review. *Carbohydr. Res.* **2020**, *494*, 108056. [CrossRef] [PubMed]

Disclaimer/Publisher's Note: The statements, opinions and data contained in all publications are solely those of the individual author(s) and contributor(s) and not of MDPI and/or the editor(s). MDPI and/or the editor(s) disclaim responsibility for any injury to people or property resulting from any ideas, methods, instructions or products referred to in the content.